ADVANCED MATERIALS

Supporting Information

for *Adv. Mater.*, DOI 10.1002/adma.202302756

Insight on the Intracellular Supramolecular Assembly of DTTO: A Peculiar Example of Cell-Driven Polymorphism

Ludovico Aloisio, Matteo Moschetta, Alex Boschi, Ariel García Fleitas, Mattia Zangoli, Ilaria Venturino, Vito Vurro, Arianna Magni, Raffaello Mazzaro, Vittorio Morandi, Andrea Candini, Cosimo D'Andrea, Giuseppe Maria Paternò, Massimo Gazzano, Guglielmo Lanzani and Francesca Di Maria**

SUPPORTING INFORMATION

Insight on the Intracellular Supramolecular Assembly of DTTO:

a Peculiar Example of Cell-Driven Polymorphism

Ludovico Aloisio, Matteo Moschetta, Alex Boschi, Ariel García Fleitas, Mattia Zangoli, Ilaria Venturino, Vito Vurro, Arianna Magni, Raffaello Mazzaro, Vittorio Morandi, Andrea Candini, Cosimo D'Andrea, Giuseppe Maria Paternò, Massimo Gazzano, Guglielmo Lanzani and Francesca Di Maria**

I. DTTO uptake

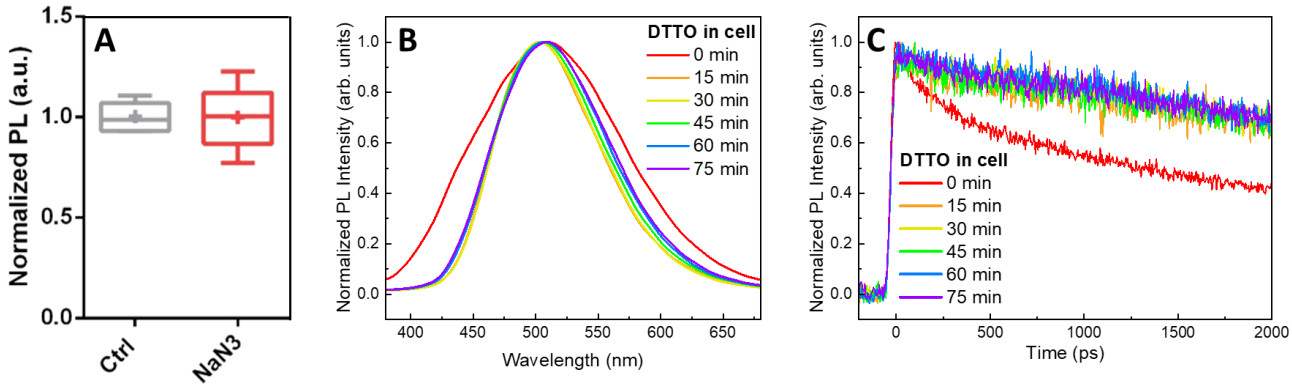

Figure S1. (A) Normalized PL intensity (at 530 nm) of the solution obtained from macerated HEK 293T cells after DTTO uptake: comparison between cells treated with NaN_3 and non-treated cells. Data are expressed as box plots. Mann-Whitney U-test; $p>0.05$; $n=6$ for both conditions. (B) Emission spectra (integrated over 2000 ps) collected from TRPL microscopy setup of DTTO upon addition to cells, monitored over time (time evolution is indicated by the color gradient of the line, from red to purple). (C) PL intensity decays of DTTO upon addition to cells, monitored over time (time evolution is indicated by the color gradient of the line, from red to purple).

As already reported in the main text, no relevant difference was found between the fluorescence signal detected from cells treated with NaN_3 and untreated ones (Figure S1A). This means that the same amount of molecule is diffused into the cell, suggesting that the uptake mechanism does not occur through an energy-dependent process but rather via diffusion of the DTTO molecule through

the cell membrane. In fact, when DTTO is diluted into DMEM, it slowly aggregates over time, and these can clearly be seen on the multiwell surface or laying on the cell membrane, unable to cross the plasma membrane, while molecular DTTO easily permeates inside the cell.

The uptake process was further investigated by monitoring the time resolved PL of cells upon DTTO addition. Cells were observed through TRPL microscopy setup, and PL signal was registered as soon as DTTO was added. As expected, upon the addition of the molecule, most of the signal comes from aggregates dispersed into the solution, resulting in a relatively short PL lifetime and broad spectra. After some time, DTTO is clearly visible inside cells, and larger aggregates have deposited on the surface of the sample. The PL decay of the signal coming from cells resembles that previously observed and does not change over time, which suggests that the monomer entering inside the cells is already well dispersed, and this remains in the absence of fiber formation. This is a further suggestion that DTTO is internalized by a simple diffusion process rather than endocytosis or other energy-dependent internalization of aggregates.

II. LSCM images of HEK-293T cells

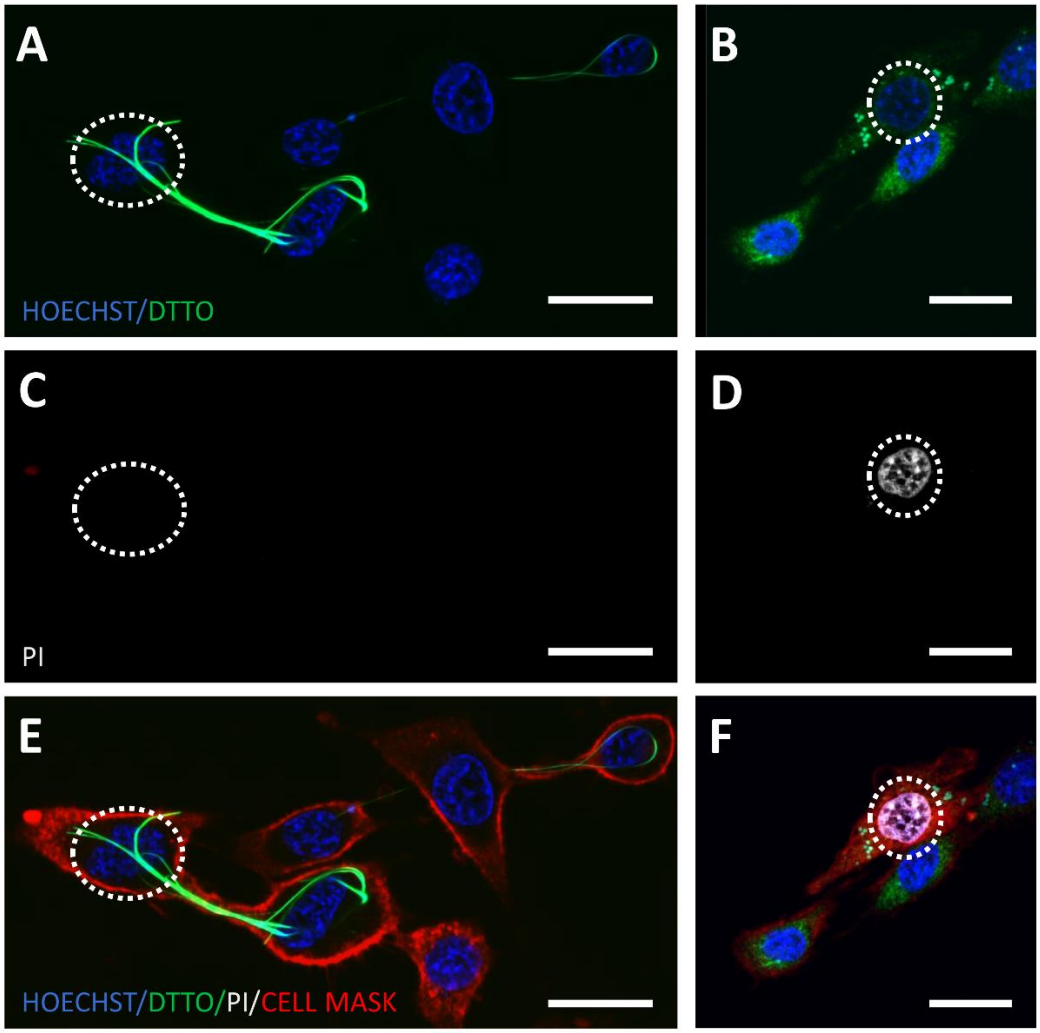

Figure S2. Laser scanning confocal microscopy (LSCM) images of C2C12 cells 24 hours after treatment with DTTO. Cells were stained for 5 minutes with Hoechst (blue, A and B) to label all the cell nuclei, propidium iodide (PI, C and D) to label the nucleus of dead cells, and CellMask™ Deep Red that stains plasma membrane. Merge images (E and F). White dotted circles indicate the nuclei of different cells. Scale bars: 20µm.

III. LSCM images of HEK-293T cells

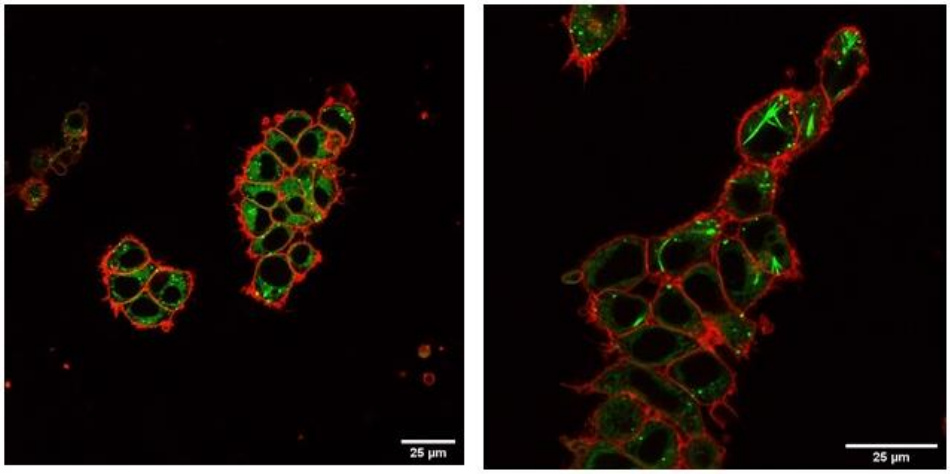

Figure S3. LSCM images of HEK-293T cells stained with DTTO, taken right after treatment (left) and after 1 hour (right).

IV. HEK 293T viability

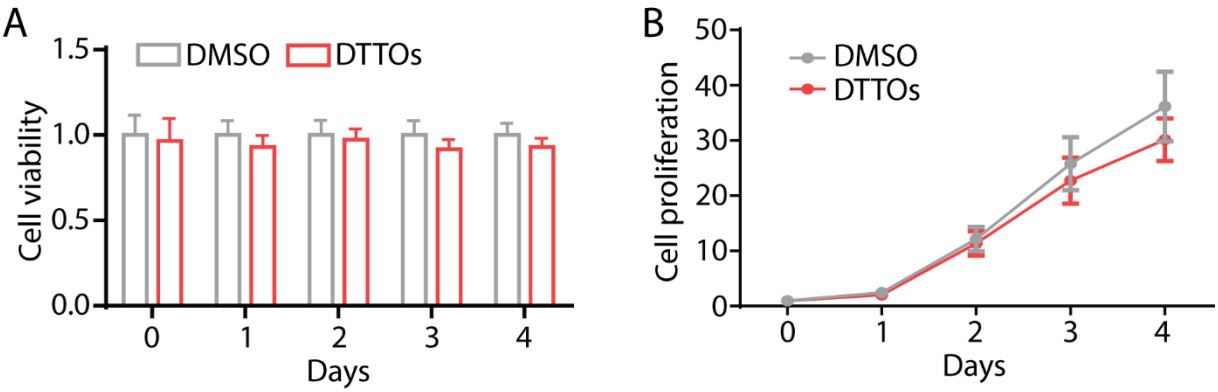

Figure S4. Normalized emission intensity at 600 nm (excitation wavelength: 546 nm) of Alamar Blue® after reacting with cells for 4 hours in complete DMEM. Emission measurements were taken by adding Alamar Blue® at 0, 1, 2, 3, and 4 days after DTTO incubation. (A) Data were normalized with respect to the average value of the control samples for each day to evaluate cell viability. (B) Data were normalized with respect to the average value of the control samples of day 0 to evaluate cell proliferation. Data are represented as mean ± sem. Two-way ANOVA/Bonferroni's test; $p>0.05$; n=12 and 11 for DMSO and DTTO, respectively.

V. Optical microscopy of DTTO aggregates

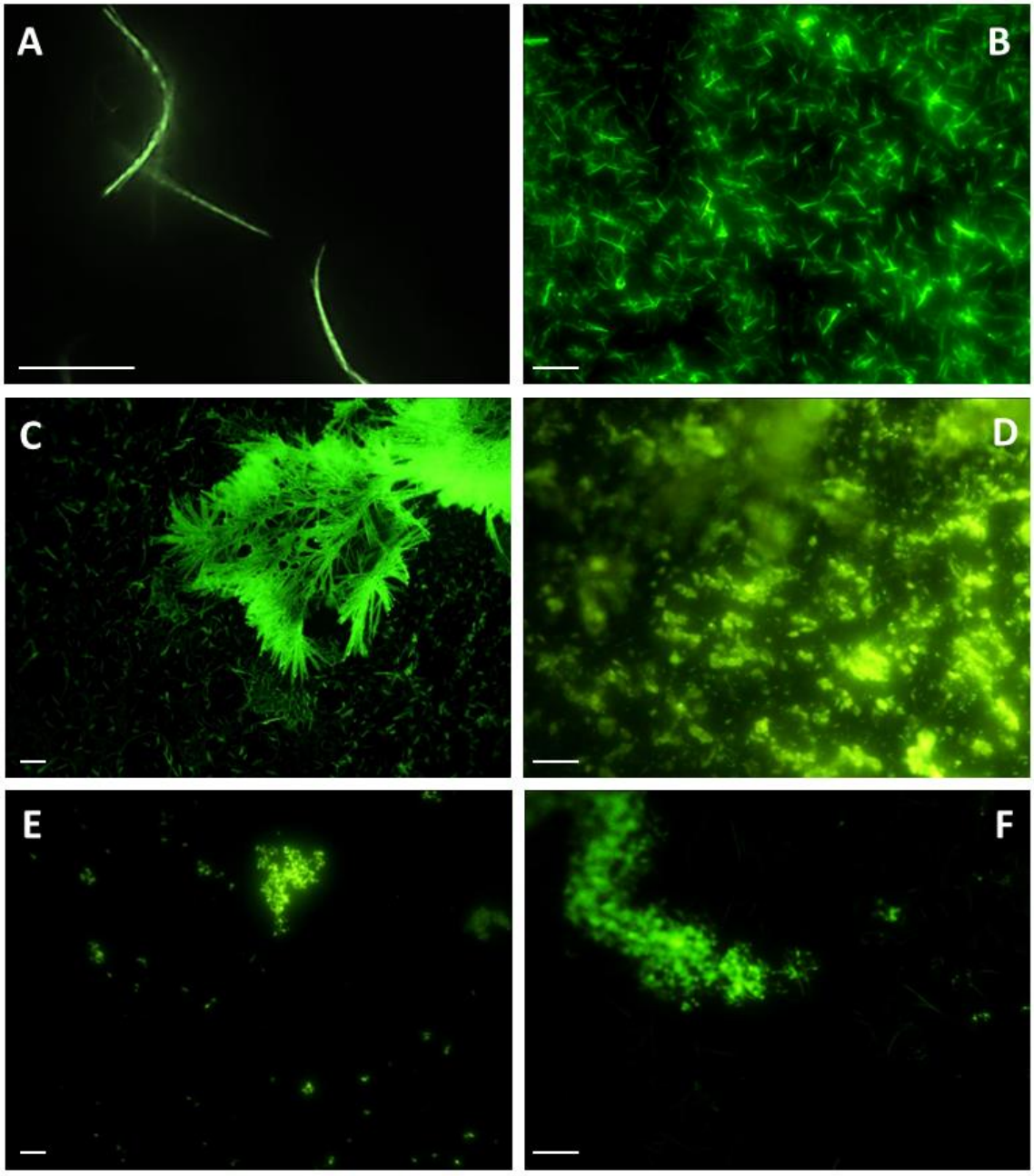

Figure S5. Aggregation of DTTO molecules in live cells (A), water (B), thin film from CH_2Cl_2 (C), DMEM (D), INTRA (E), KRH (F). Scale bars: 25 μm.

VI. SEM images of fibers

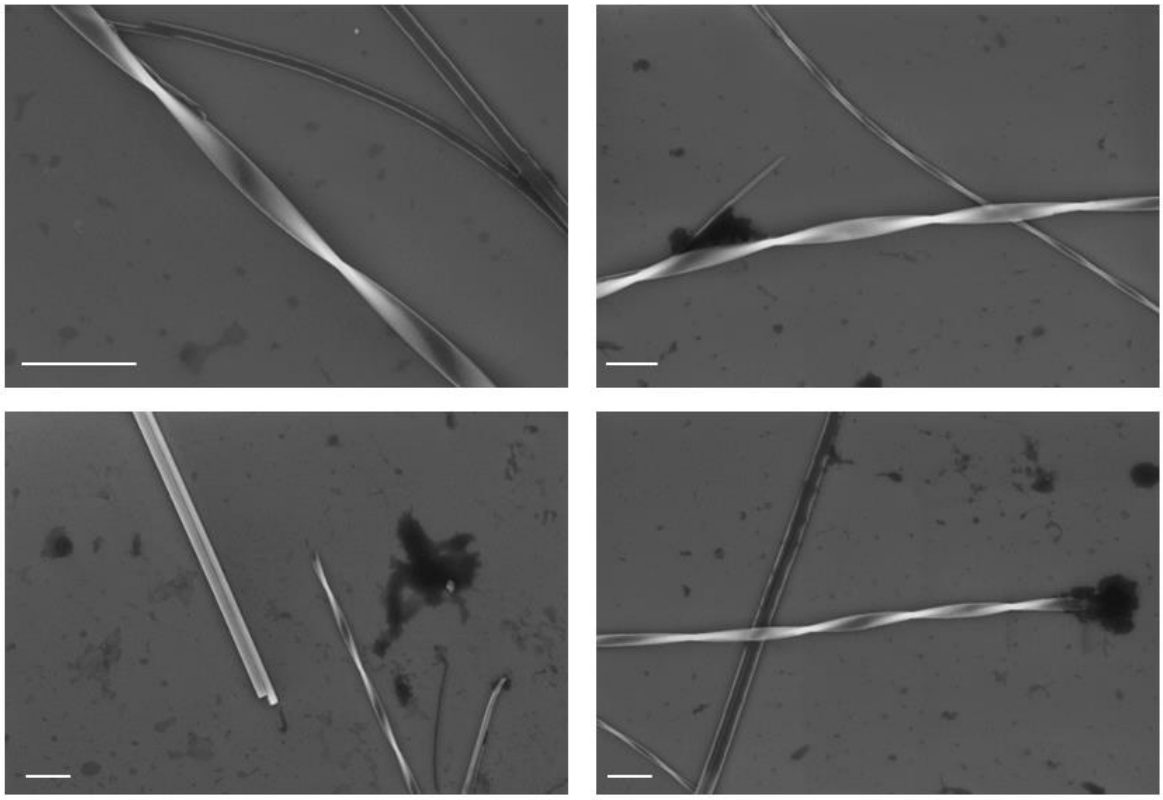

Figure S6. SEM images of helicoidal and straight fibers. Scale bars: 1 µm.

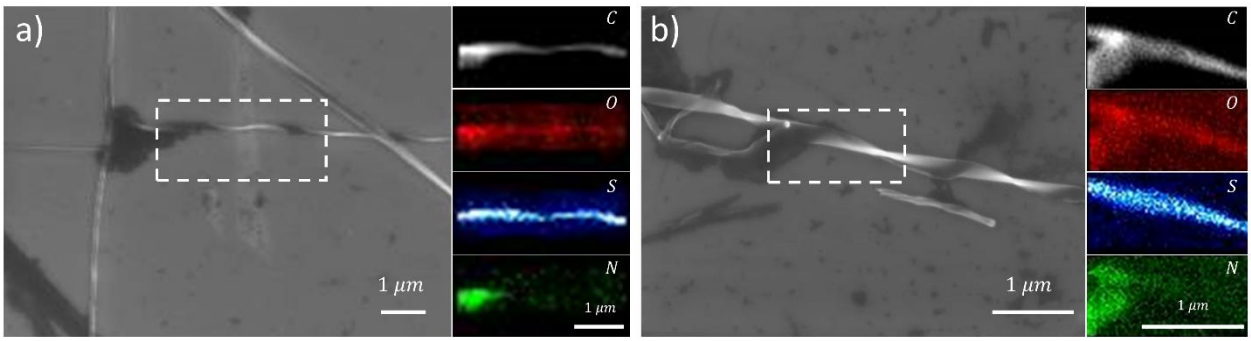

Figure S7. Additional FE-SEM images of DTTO fibers and EDS mapping of the selected area, highlighting the presence of a N-rich coating corresponding to the high contrast area on SEM images.

VII. Raman microscopy

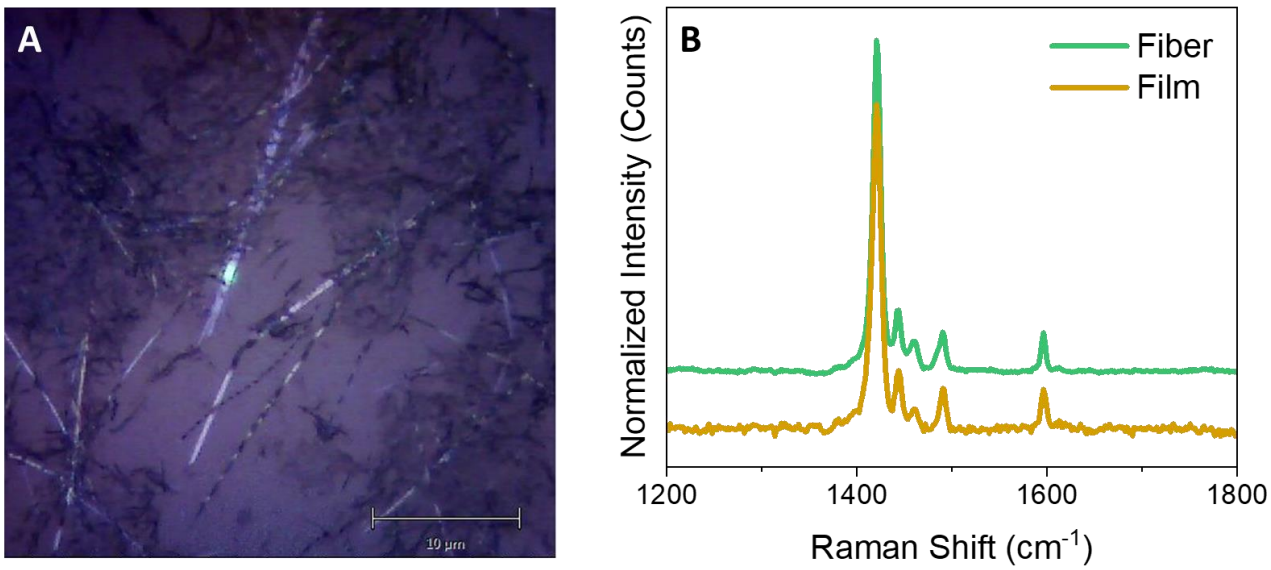

Figure S8. (A) Fibers deposited on a glass substrate, seen with 50X objective microscope coupled with Raman spectroscopy setup. Excitation laser spot is visible in green. (B) Raman shift spectra of (top) drop casted DTTO film and (bottom) isolated fibers, excitation 532 nm.

VIII. Relative photoluminescence quantum yield

The addition of a dithienothiophene moiety as an internal core renders the structure of the molecule highly rigid, dramatically enhancing the PL quantum yield in solution with respect to other oligothiophenes.[18] In fact, DTTO diluted in DMSO was previously reported to have a quantum yield of 0.85 in solution.[19]

As expected, aggregation of DTTO leads to a reduction of PL due to the rise of non-radiative relaxation pathways. As depicted in Figure S7, relative PLQY was established at an average of 5% for DTTO in water and 9% for the thin film. It is interesting to note that the QY of films is almost doubled, suggesting that a more ordered crystalline structure plays a role in PL efficiency. More curiously, fibers showed a higher QY with respect to the other aggregate structures: 35% for fibers in solutions and 33% for a drop casted film of fibers. This suggests again that DTTO in fibers has an aggregation order which strongly differs from the others analyzed.

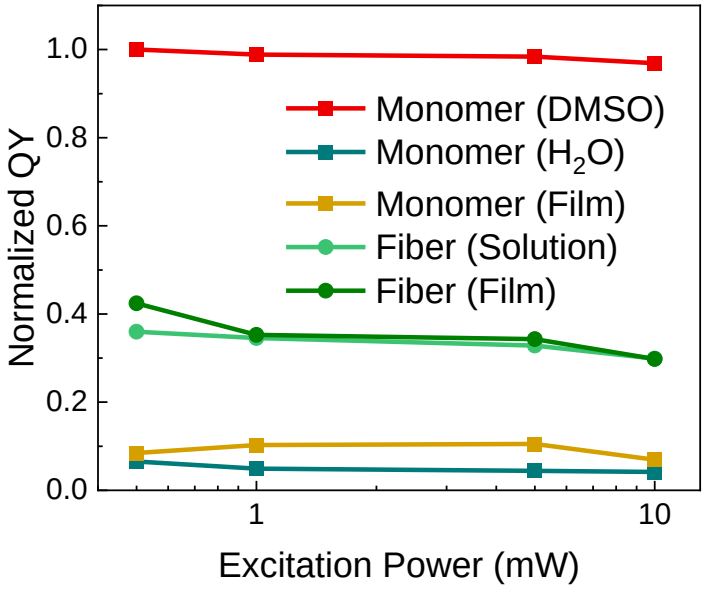

Figure S9. Relative QY of DTTO in solution (red and blue), fibers dispersed in lysis buffer (light green), fibers deposited on glass substrate (dark green), and in solid state (yellow) with respect to the molecule diluted in DMSO. QY was measured following the protocol reported by de Mello et al.[17] and was normalized with respect to the maximum efficiency measured.

IX. PL spectra and lifetimes of DTTO fibers before and after isolation from cells

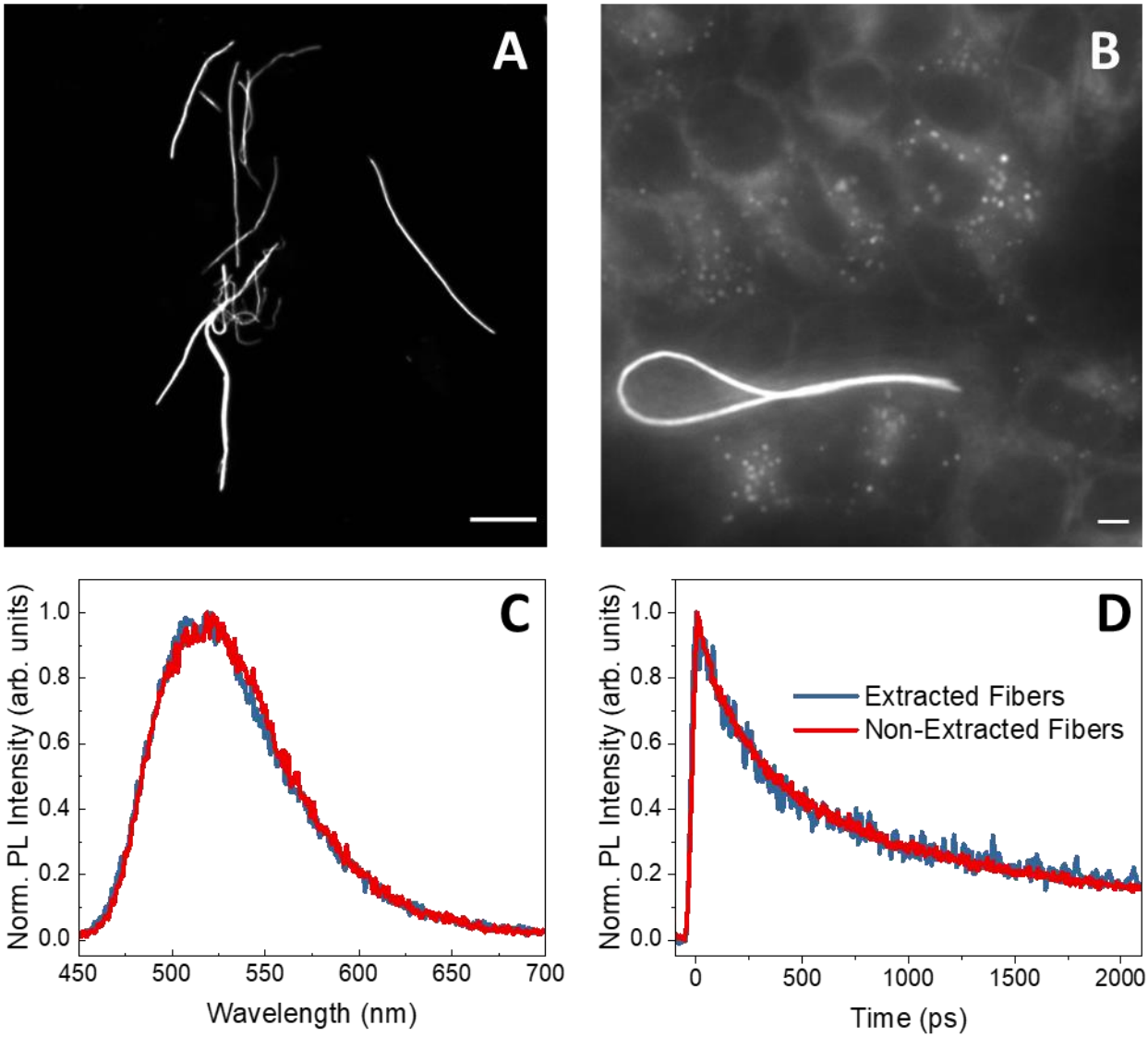

Figure S10. PL spectra and decays of fibers before and after extraction.

X. PL anisotropy decays of DTTO film and fibers

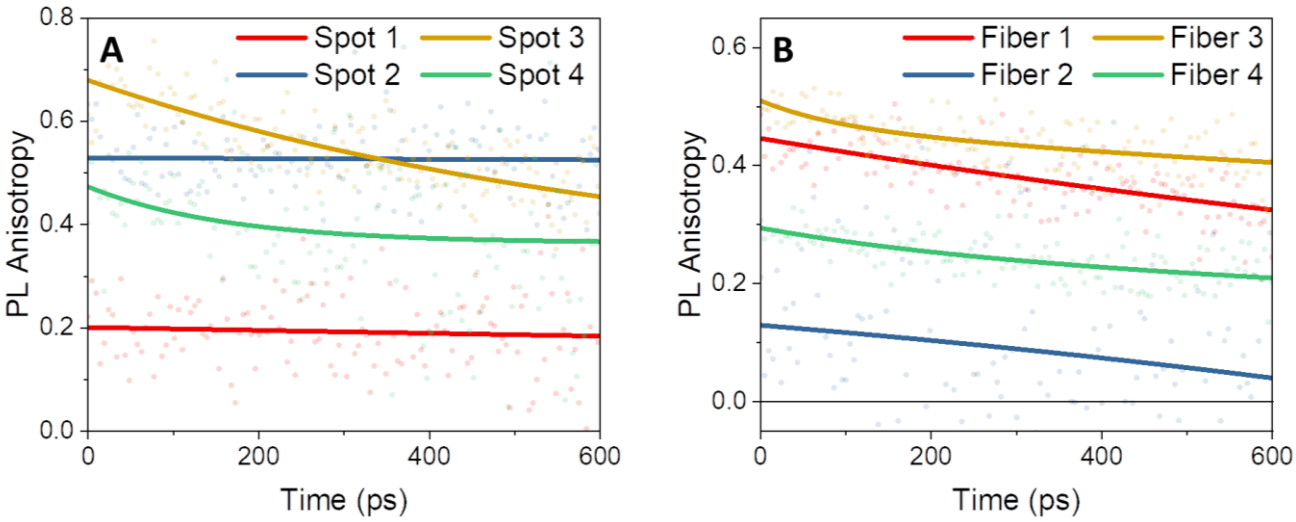

Figure S11. PL anisotropy decays measured on (A) different spots of a DTTO thin film and (B) different, randomly oriented, DTTO fibers.

XI. DTTO molecules orientation in fibers

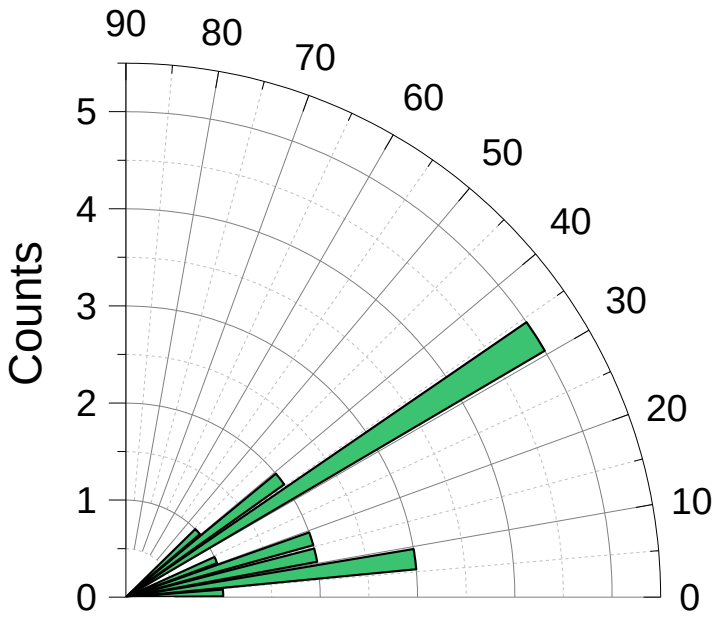

Figure S12. Angle between calculated absorption/emission fluorescence dipole moment of DTTO molecule and fiber orientation.

XII. XRD of DTTO aggregates

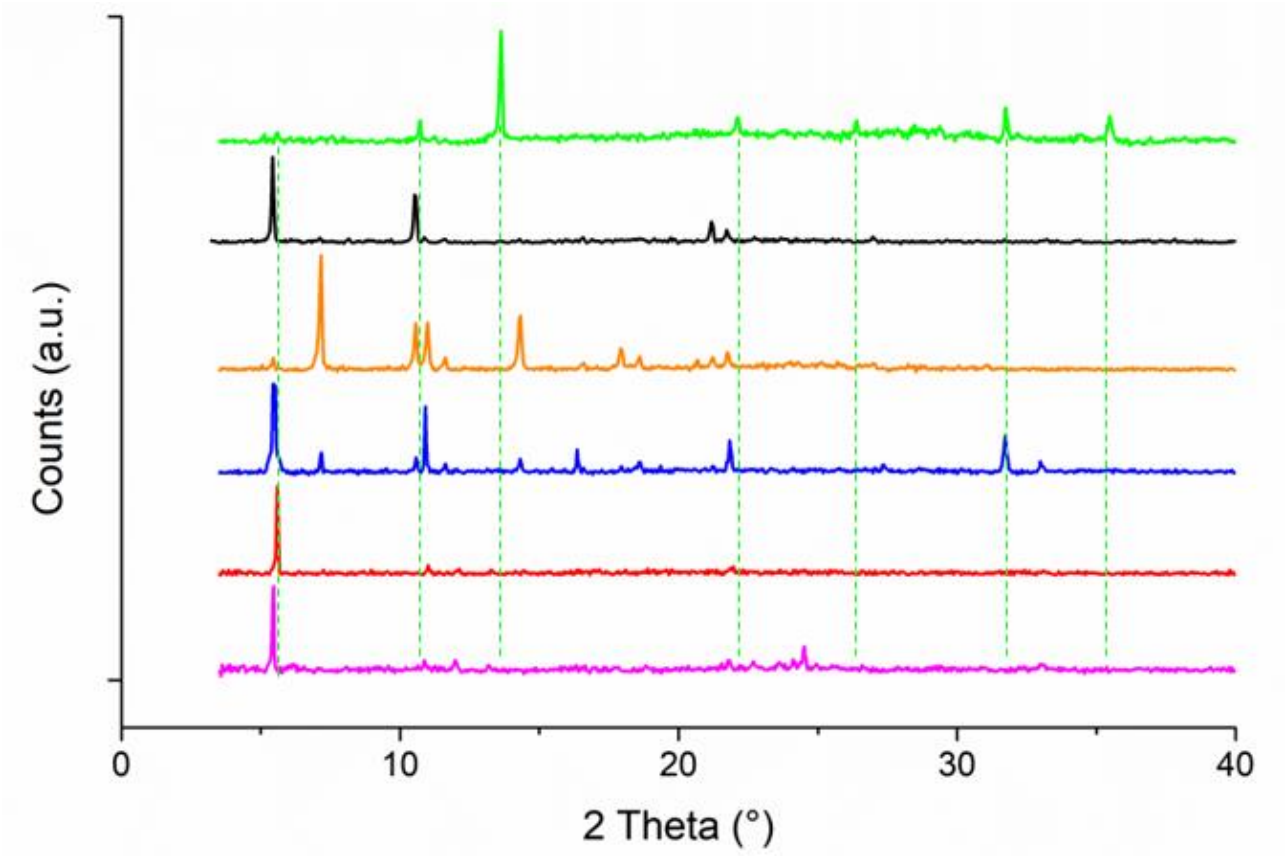

Figure S13. XRD patterns of scans obtained from fiber (green line) and DTTO films from water (black line), CH_2Cl_2 (orange line), KRH (blue line) DMEM (red line), and INTRA (magenta line). The bell shaped background due to the amorphous component of the support was subtracted. Dashed lines are simply a guide for the eyes.

XIII. PL Intensity decay of DTTO in different matrices

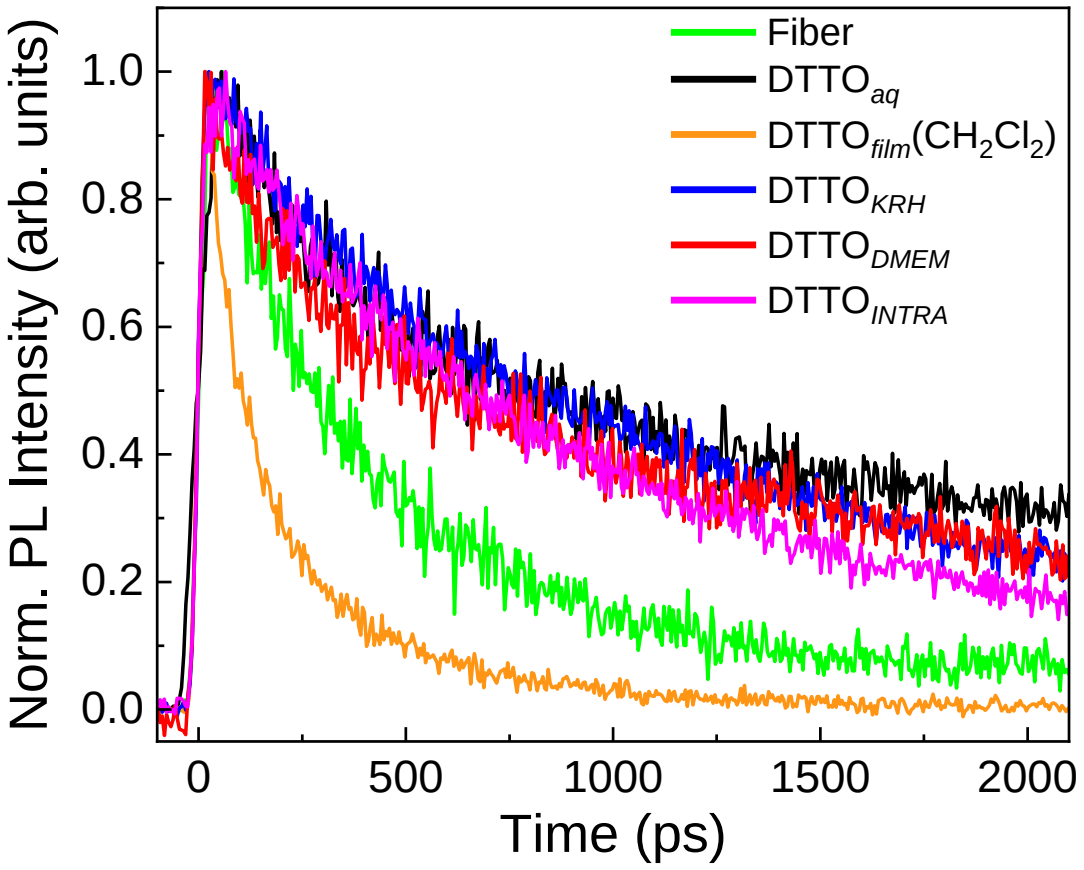

Figure S14. PL signal decay over time of DTTO in fibers, film drop casted from CH_2Cl_2 and DTTO diluted in different matrices: H_2O (black line), KRH (blue line), DMEM (red line) and Intracellular solution (magenta line).

XIV. AFM image of DTTO thin film

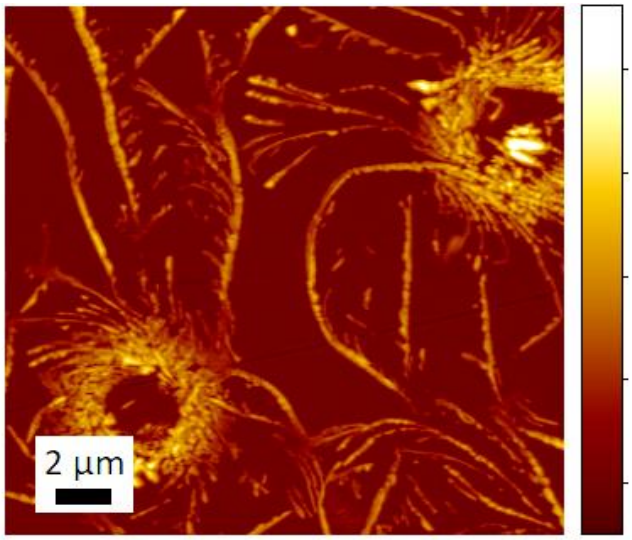

Figure S15. Topography image obtained by scanning probe microscopy of DTTO thin film.

XV. DTTO fibers in myotubes

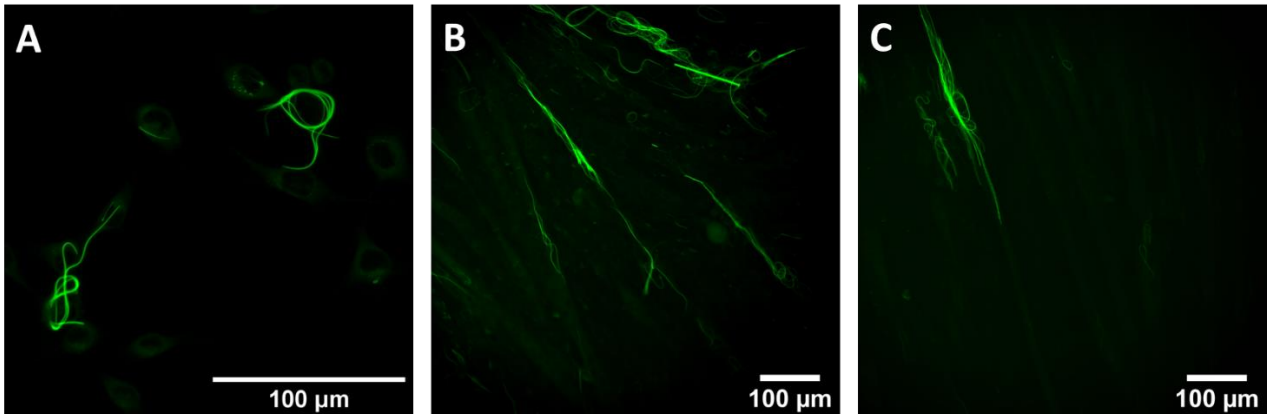

Figure S16. LSCM images of (A) C2C12 myoblasts and (B, C) C2C12 myotubes 2 days after incubation with DTTO.

XVI. DTTO fibers in myotubes

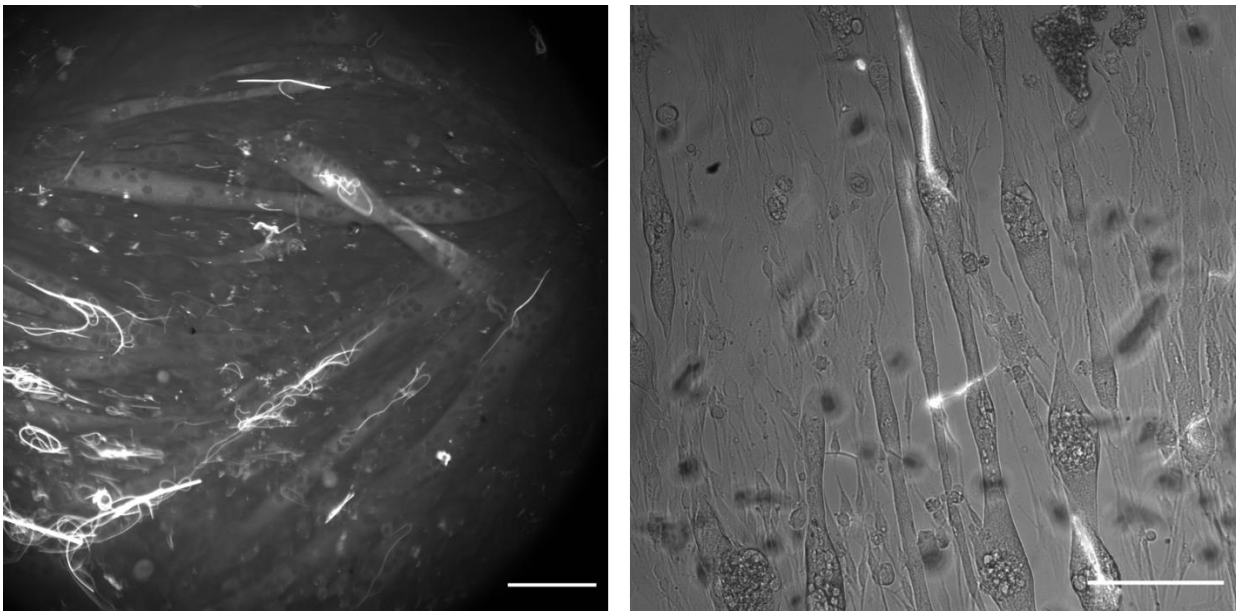

Figure S17. Fluorescence microscopy pictures of DTTO fibers formed in myotubes crossing the cell membranes. Scale bars: 100 µm.

XVII. Videos

Video V1. Series of Z-stack images from bottom to top of HEK-293T cells depicting the growth of a DTTO fiber.

Video V2. Contraction of C2C12 myotube containing DTTO fibers.